

Some Results Concerning the Viscoelastic Relaxation of Prestress in a Surface Rock Anchor

A. P. S. SELVADURAI*

This paper investigates the axisymmetric interactive behaviour of a rigid circular plate anchored to a halfspace region susceptible to creep. The anchoring load corresponds to a distribution of Mindlin type forces, of finite length, located along the axis of symmetry. The creep behaviour of the halfspace region is represented by a linear viscoelastic material with elastic dilatational behaviour and distortional behaviour of the three-parameter solid type. Using this particular idealization, solutions are developed for the loss of prestress in an anchor bolt subjected to a displacement which is a step function of time. The prestress load at the anchor region is assumed to be distributed in a uniform, linear or parabolic fashion. The numerical results presented herein illustrate the manner in which the decay of the prestress load can be influenced by the length, depth of location and load distribution in the anchor region and the creep characteristics of the halfspace region.

INTRODUCTION

The time-dependent effects associated with the performance of ground and rock anchors is of interest to many engineering problems (see for example Lang [1] and Gosschalk and Taylor [2]). The influence of such time-dependent effects on the behaviour of a rigid spheroidal anchor region embedded in bonded contact with a linear viscoelastic medium was examined by Selvadurai [3]. The above treatment of the problem in linear viscoelasticity theory was facilitated by the application of a Laplace transform based correspondence principle. Using such a technique, analytical solutions were developed for the time-dependent decay of a prestress load. It was shown that linear viscoelastic modelling of the anchor problem provides a useful first approximation for the examination of anchors embedded in creep-susceptible geological materials such as granite, sandstone, limestone, etc.

This paper extends the above line of investigation to include the behaviour of a rigid circular plate which is anchored to a viscoelastic halfspace. In particular, we consider the axisymmetric interaction of a rigid circular plate resting in smooth contact with a linear viscoelastic halfspace which is, in turn, loaded internally by a distribution of Mindlin forces of finite length located at a finite depth along the axis of symmetry (Fig. 1). The particular distributions of Mindlin forces consist of uniform, linear or parabolic variations as shown in

Fig. 1. In order to apply the correspondence principle to the analysis of the linear viscoelasticity problem we first require the solution of the analogous problem in the classical theory of isotropic elasticity. (The latter then corresponds to the viscoelastic solution in the transformed space.) Such a solution can be developed by using the dual integral equation [4,5] or complex potential function [6-8] approach developed for the analysis of mixed boundary value problems in classical elasticity theory. Since the effects that are of importance

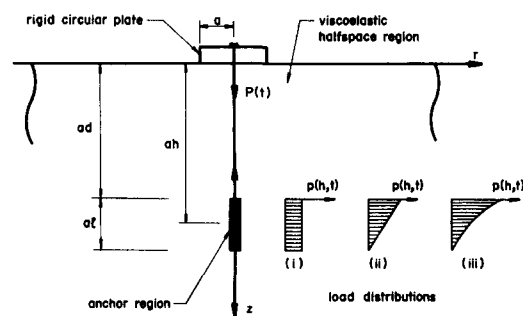


Fig. 1. The rigid plate-anchor system. Anchor load distribution $p(h, t)$.

$$(i) \quad p(h, t) = \frac{P(t)}{2a};$$

$$(ii) \quad p(h, t) = \frac{2P(t)}{l^2 a} \{l + d - h\};$$

$$(iii) \quad p(h, t) = \frac{P(t)}{l^3 a} \{l + d - h\}^2$$

where $P(t)$ is the anchor load.

* Department of Civil Engineering, Carleton University, Ottawa, Canada.

to the viscoelasticity problem are of the load-settlement-time type, it is more convenient to adopt the latter approach. Using the complex potential function approach, a solution is first developed to the problem of the axisymmetric smooth interaction of a rigid circular plate under the simultaneous action of an external force and an internal concentrated Mindlin [9] force. It is found that the solutions for the resultant rigid displacement experienced by the plate together with the contact stress generated at the smooth plate-elastic halfspace interface can be evaluated in exact closed forms. Since it is assumed that the bearing plate is not bonded to the halfspace it is incapable of sustaining tensile tractions. The solution developed for the contact stress can then be used to examine the critical depth of location of the anchoring force at which tension occurs at the interface. The expressions developed for the internal concentrated force can be integrated to generate solutions for other types of distributed internal line loads. Since only tractions are prescribed at the anchor locations it is understood that the anchor region is perfectly flexible.

The solution to the viscoelasticity problem can be obtained by inversion of the corresponding elastic solution in which the elastic constants are replaced by their transformed viscoelastic equivalents. Details of the application of the correspondence principle together with references to the original studies are given in [3]. In the present paper explicit solutions are presented for the time-dependent interaction problem in which the viscoelastic halfspace region exhibits a dilatational behaviour which is elastic and a deviatoric behaviour which is of the three-parameter solid type [10]. Typical values encountered in the classification of many geological materials according to this particular viscoelastic idealization are listed in a later section. The numerical results presented, illustrate the load relaxation behaviour of an anchored plate or a rock bolt system which is subjected to a step function of displacement. These numerical results indicate the manner in which (i) the depth of location of the anchor region, (ii) the length of the anchor region, (iii) the nature of load distribution in the anchor region, and (iv) the viscoelastic characteristics of the halfspace region influence the rate of decay of load in a prestressed anchored plate.

TRANSFORMED RESULTS OF LINEAR VISCOELASTICITY IN CYLINDRICAL POLAR COORDINATES

We consider the class of axisymmetric problems referred to a cylindrical polar coordinate system (r, θ, z) . The transformed deformation field $\bar{u}(r, z, s)$ has components

$$\bar{u}(r, z, s) = \{\bar{u}_r(r, z, s), 0, \bar{u}_z(r, z, s)\} \quad (1)$$

where s is the transform parameter. The transformed components of the stress tensor $(\bar{\sigma}_{ij})$ and the strain

tensor $(\bar{\epsilon}_{ij})$ are defined as follows:

$$\bar{\sigma}_{ij}(r, z, s) = \begin{bmatrix} \bar{\sigma}_{rr} & 0 & \bar{\sigma}_{rz} \\ 0 & \bar{\sigma}_{\theta\theta} & 0 \\ \bar{\sigma}_{rz} & 0 & \bar{\sigma}_{zz} \end{bmatrix};$$

$$\bar{\epsilon}_{ij}(r, z, s) = \begin{bmatrix} \bar{\epsilon}_{rr} & 0 & \bar{\epsilon}_{rz} \\ 0 & \bar{\epsilon}_{\theta\theta} & 0 \\ \bar{\epsilon}_{rz} & 0 & \bar{\epsilon}_{zz} \end{bmatrix} \quad (2)$$

The transformed equivalents are defined by

$$[\bar{\sigma}_{ij}(r, z, s); \bar{\epsilon}_{ij}(r, z, s)] \\ = \int_0^\infty [\sigma_{ij}(r, z, t); \epsilon_{ij}(r, z, t)] e^{-st} dt$$

The viscoelastic stress-strain-time relations can be represented in terms of the relaxation integral laws

$$S_{ij}(r, z, t) = \int_{-\infty}^t J_1(t - \tau) \frac{\partial}{\partial \tau} e_{ij}(r, z, \tau) d\tau \quad (3a)$$

and

$$\sigma_{kk}(r, z, t) = \int_{-\infty}^t J_2(t - \tau) \frac{\partial}{\partial \tau} \epsilon_{kk}(r, z, \tau) d\tau \quad (3b)$$

where

$$S_{ij} = \sigma_{ij} - \frac{1}{3} \delta_{ij} \sigma_{kk}; \quad e_{ij} = \epsilon_{ij} - \frac{1}{3} \delta_{ij} \epsilon_{kk}$$

and $J_\alpha (\alpha = 1, 2)$ are the relaxation moduli in shear and isotropic compression respectively. The transformed viscoelastic equivalents of the shear modulus $G(t)$ and Poisson's ratio $\nu(t)$ can be expressed in terms of $J_\alpha (\alpha = 1, 2)$ as follows [10]:

$$\bar{G}(s) = 2sJ_1(s); \quad \bar{\nu}(s) = \frac{\bar{J}_2(s) - \bar{J}_1(s)}{\bar{J}_1(s) + 2\bar{J}_2(s)} \quad (4)$$

In the present analysis, attention is restricted to the viscoelastic behaviour which is represented by the following dilatational and distortional responses:

$$\sigma_{kk} = 3\phi G_0 \epsilon_{kk} \quad (5a)$$

$$\left[\frac{\partial}{\partial t} + \frac{G_0(1 + \tilde{\alpha})}{\eta} \right] S_{ij} = \left[G_0 \frac{\partial}{\partial t} + \frac{G_0^2 \tilde{\alpha}}{\eta} \right] e_{ij} \quad (5b)$$

where $G_0, \tilde{\alpha}, \eta$ and ϕ are material constants. Some typical values for these, derived for creep susceptible geological materials such as granite, sandstone, limestone etc., are shown in Table 1. For the viscoelastic behaviour characterized by (5) we note that [3]

$$\bar{J}_1(s) = \frac{G_0[s + (\tilde{\alpha}G_0/\eta)]}{s[s + (1 + \tilde{\alpha})(G_0/\eta)]}; \quad \bar{J}_2(s) = \frac{3\phi G_0}{s} \quad (6)$$

THE COMPLEX POTENTIAL FUNCTION APPROACH

The complex potential function approach for the solution of problems in classical elasticity was first proposed by Green [6] and comprehensive accounts of the associated analytical developments are given by

TABLE 1. TYPICAL VISCOELASTIC PARAMETERS FOR GEOLOGICAL MATERIALS [3]

Material	$G_0(\text{MN/m}^2)$	$\eta(\text{MNhr/m}^2)$	ϕ	α	$\tau(\text{hr})$	Symbol
Granite	7.0×10^4	1.0×10^8	0.69	12.0	119.0	○
Sandstone	6.0×10^4	1.5×10^7	0.50	9.0	27.8	□
Limestone	5.6×10^4	4.4×10^7	0.90	6.0	130.9	×
Mudstone	3.5×10^4	6.0×10^6	0.57	2.0	85.7	△
Concrete	2.9×10^4	2.2×10^6	0.80	0.6	126.4	●
Shale	1.0×10^4	2.7×10^6	2.00	0.2	1350.0	■
Rocksalt	7.0×10^3	2.0×10^4	0.85	0.3	9.5	+
Potash	3.8×10^3	6.4×10^5	1.31	0.5	336.8	▲

Green and Zerna [7] and Collins [8]. In the context of the transformed problem in linear viscoelasticity theory, it can be shown that the class of problems related to a halfspace region ($z \geq 0$) in which the shear stresses vanish on $z = 0$, can be reduced to classical problems in potential theory. The transformed equivalents of the displacement and stress components can be uniquely represented in terms of a single potential function $\bar{\Phi}(r, z, s)$. For example, the transformed stress components $\bar{\sigma}_{zz}(r, z, s)$, $\bar{\sigma}_{rz}(r, z, s)$ and the displacement component $\bar{u}_z(r, z, s)$ can be represented in the forms

$$\begin{aligned} 2\bar{G}(s)\bar{u}_z(r, z, s) &= \left[z \frac{\partial}{\partial z} - 2\{1 - \bar{\nu}(s)\} \right] \bar{\Phi}(r, z, s) \\ \bar{\sigma}_{zz}(r, z, s) &= \left[z \frac{\partial^3}{\partial z^3} - \frac{\partial^2}{\partial z^2} \right] \bar{\Phi}(r, z, s) \\ \bar{\sigma}_{rz}(r, z, s) &= z \frac{\partial^2 \bar{\Phi}}{\partial z^2}(r, z, s) \end{aligned} \quad (7)$$

where $\bar{G}(s)$ and $\bar{\nu}(s)$ are the transformed equivalents of the linear elastic shear modulus and Poisson's ratio. The transformed boundary conditions associated with the interaction problem are

$$\begin{aligned} \bar{u}_z(r, 0, s) &= \frac{1 - \bar{\nu}(s)}{\bar{G}(s)} \frac{\partial \bar{\Phi}}{\partial z} = \bar{u}^*(r, s) \quad \text{on } r \leq a \\ \bar{\sigma}_{zz}(r, 0, s) &= -\frac{\partial^2 \bar{\Phi}}{\partial z^2} = 0 \quad \text{on } r \geq a \end{aligned} \quad (8)$$

and the boundary condition pertaining to $\bar{\sigma}_{rz}(r, 0, s) = 0$, is automatically satisfied by the form of $\bar{\sigma}_{rz}(r, z, s)$ given by (7). Consider the representation

$$-\frac{1 - \bar{\nu}(s)}{\bar{G}(s)} \frac{\partial \bar{\Phi}}{\partial z}(r, z, s) = \frac{1}{2} \int_{-a}^a \frac{\bar{g}(\lambda, s) d\lambda}{[r^2 + (z + i\lambda)^2]^{1/2}} \quad (9)$$

which satisfies $\nabla^2 \bar{\Phi}(r, z, s) = 0$, and the regularity conditions at infinity (a is the radius of the circular plate). It can then be shown that the boundary conditions (8) can be reduced to the single integral equation

$$\bar{u}^*(r, s) = \int_0^r \frac{\bar{g}(\lambda, s) d\lambda}{[r^2 - \lambda^2]^{1/2}} \quad (10)$$

in terms of the unknown function $\bar{g}(\lambda, s)$. The Abel integral equation of the second kind (10), can be inverted to complete the transformed solution. Assuming

that $\bar{u}^*(r, s)$ is continuously differentiable in the region $r \leq a$ for all $t \geq 0$, the solution of (10) is given by

$$\bar{g}(\lambda, s) = \frac{2}{\pi} \frac{d}{d\lambda} \int_0^\lambda \frac{r \bar{u}^*(r, s) d\lambda}{[\lambda^2 - r^2]^{1/2}} \quad (11)$$

The transformed result for the contact stress distribution ($\bar{\sigma}_{zz}$) at the interface can be expressed in terms of $\bar{g}(\lambda, s)$ in the form

$$\bar{\sigma}_{zz}(r, 0, s) = \frac{\bar{G}(s)}{\{1 - \bar{\nu}(s)\}} \frac{1}{r} \frac{\partial}{\partial r} \int_r^a \frac{\lambda \bar{g}(\lambda, s) d\lambda}{[\lambda^2 - r^2]^{1/2}} \quad (12)$$

Also, the transformed result for the total force exerted by the rigid circular plate can be represented in the form

$$\bar{P}(s) = \frac{2\pi \bar{G}(s)}{\{1 - \bar{\nu}(s)\}} \int_0^a \bar{g}(\lambda, s) d\lambda \quad (13)$$

INTERACTION BETWEEN THE RIGID CIRCULAR PLATE AND THE INTERNAL ANCHOR LOADS

We first consider the transformed axisymmetric problem of the smooth contact between a rigid circular plate subjected simultaneously to an external load [with a transformed equivalent of $\bar{P}(s)$] and an internal concentrated Mindlin force [with a transformed equivalent $\bar{P}_0(s)$] which acts at a distance c (in the negative z -direction) along the axis of symmetry. We assume that there is no loss of contact at the rigid plate—viscoelastic halfspace interface due to the combined action of the transformed loads $\bar{P}(s)$ and $\bar{P}_0(s)$. The transformed value of the resultant displacement of the circular plate is denoted by $\bar{w}_0(s)$. Considering the result given by Mindlin [9] for the internal concentrated force in an isotropic elastic halfspace, it can be shown that the function $\bar{u}^*(r, s)$ is given by

$$\begin{aligned} \bar{u}^*(r, s) &= \bar{w}_0(s) + \frac{\bar{P}_0(s)\{1 - \bar{\nu}(s)\}}{2\pi \bar{G}(s)} \\ &\times \left\{ \frac{1}{(r^2 + c^2)^{1/2}} + \frac{c^2}{2\{1 - \bar{\nu}(s)\}(r^2 + c^2)^{3/2}} \right\} \end{aligned} \quad (14)$$

Considering (7) and (10) we obtain

$$\bar{g}(\lambda, s) = \frac{2}{\pi} \left[\bar{w}_0(s) + \frac{\bar{P}_0(s)c}{4\pi\bar{G}(s)} \right] \times \left\{ \frac{[3 - 2\bar{v}(s)]}{(\lambda^2 + c^2)} - \frac{2\lambda^2}{(\lambda^2 + c^2)^2} \right\} \quad (15)$$

Using (15) in (12) we obtain the following expression for the transform of the displacement of the rigid circular plate:

$$\bar{w}_0(s) = \frac{\bar{P}[1 - \bar{v}(s)]}{4a\bar{G}(s)} \left[1 - \frac{\bar{P}_0(s)}{\bar{P}(s)} \right] \times \left\{ \frac{2}{\pi} \tan^{-1} \left(\frac{a}{c} \right) + \frac{ac}{\pi[1 - \bar{v}(s)](a^2 + c^2)} \right\} \quad (16)$$

We note that as $c \rightarrow 0$, (16) reduces to the transformed equivalent of the classical Boussinesq problem. Also when $c \rightarrow 0$ and $\bar{P}(s) = \bar{P}_0(s)$ for all $t \geq 0$, the rigid plate is subjected to a doublet of forces; as such, $\bar{w}_0(s) = 0$. The contact stress distribution at the interface of the plate $\bar{\sigma}_{zz}(r, 0, s)$ is given by

$$\bar{\sigma}_{zz}(r, 0, s) = -\frac{\bar{P}(s)}{2\pi a[a^2 - r^2]^{1/2}} \left[1 + \frac{\bar{P}_0(s)}{\bar{P}(s)} \bar{T}(r, c, s) \right] \quad (17)$$

where

$$\begin{aligned} \bar{T}(r, c, s) = & -\left\{ \frac{2}{\pi} \tan^{-1} \left(\frac{a}{c} \right) + \frac{ac}{\pi[1 - \bar{v}(s)](a^2 + c^2)} \right\} \\ & + \frac{ac}{\pi[1 - \bar{v}(s)](r^2 + c^2)^2} \\ & \times \left\{ [1 - 2\bar{v}(s)](r^2 + c^2) + c^2 \right. \\ & + \frac{c^2\{2a^2 + c^2 - r^2\}}{(a^2 + c^2)} \\ & + ([1 - 2\bar{v}(s)](r^2 + c^2) + 3c^2) \\ & \left. \times \sqrt{\frac{a^2 - r^2}{r^2 + c^2}} \tan^{-1} \sqrt{\frac{a^2 - r^2}{r^2 + c^2}} \right\} \quad (18) \end{aligned}$$

[We note that the negative sign of (17) indicates a compressive stress.] From (18) it is evident that the contact stress distribution at the interface is time-dependent. As $c \rightarrow \infty$, (17) reduces to the Boussinesq equivalent which is essentially time-independent when $\bar{P} = \text{const.}$, for all $t \geq 0$. The closed form solution (16) developed for the displacement of the rigid circular plate under the action of the internal concentrated force can be used to generate the solutions for other types of distributed internal loads located along the axis of symmetry. Three particular forms of internal load distributions are examined (Fig. 1); the anchoring load $\bar{P}_0(s)$ ($= \bar{P}(s)$) is assumed to be distributed either (i) uniformly, (ii) linearly, or (iii) parabolically over a finite length. An integration of (16) within the appropriate limits yields exact closed form solutions for all

of the above cases. In general, the transformed displacement of the distributed axisymmetric internal line loadings can be represented in the form

$$\bar{w}_0(s) = \frac{\bar{P}(s)}{4a\bar{G}(s)} [\{1 - A_1(l, d)\} \{1 - \bar{v}(s)\} - A_2(l, d)] \quad (19)$$

where $A_i(l, d)$, ($i = 1, 2$) are functions which depend on the depth of location of the anchor (ad), its length (al) and on the type of internal load distribution. The relevant expressions for A_i , valid for the three distributions of internal loading discussed above, are given in Appendix 1.

VISCOELASTIC RELAXATION OF PRESTRESS

The result relating the transformed displacement $\bar{w}_0(s)$ and the transformed load $\bar{P}(s)$, (16), can be used to determine the viscoelastic relaxation of prestress in the anchor-rigid plate system. We assume that the anchored rigid circular plate is subjected to the displacement field

$$w_0(t) = w_0^* H(t) \quad (20)$$

where $H(t)$ is the Heaviside step function. By using the expressions for $\bar{G}(s)$ and $\bar{v}(s)$ [obtained from (4) and (6)] together with $\bar{w}_0(s) (= w_0^*/s)$ in (19) we obtain the following expression for the transformed prestress load $\bar{P}(s)$ in the anchor-plate system: we have

$$\begin{aligned} \frac{\bar{P}(s)}{8a\omega_0^* G_0} = & \frac{1}{[K_3 \{1 - A_1(l, d)\} - A_2(l, d)]} \\ & \times \left\{ \frac{(\tau s + \zeta_1)(\tau s + K_2)}{s(\tau s + \zeta_2)(\tau s + \zeta_3)} \right\} \quad (21) \end{aligned}$$

where

$$\zeta_1 = 1; \quad \zeta_2 = \frac{1 + \tilde{\alpha}}{\tilde{\alpha}};$$

$$\zeta_3 = \frac{K_1 K_3 \{1 - A_1(l, d)\} - K_2 A_2(l, d)}{K_3 \{1 - A_1(l, d)\} - A_2(l, d)}$$

$$K_1 = \frac{2\zeta_1 + 3\phi\zeta_2}{2\zeta_1 + 3\phi}; \quad K_2 = \frac{\zeta_1 + 6\phi\zeta_2}{\zeta_1 + 6\phi};$$

$$K_3 = \frac{3\phi + 2\zeta_1}{6\phi + \zeta_1} \quad (22)$$

and $\tau (= \eta/\tilde{\alpha}G_0)$ is the retardation time in the deviatoric response. Taking the inverse transform of the result (21) we obtain the load relaxation behaviour in the anchor-circular plate system; i.e.

$$\frac{P(t)}{8a\omega_0^* G_0} = \frac{R(t)}{[K_3 \{1 - A_1(l, d)\} - A_2(l, d)]} \quad (23a)$$

where

$$\begin{aligned}
 R(t) = & \frac{\zeta_1 K_2}{\zeta_2 \zeta_3} \{1 - e^{-\zeta_2 t/\tau}\} \\
 & + \left\{ \frac{\zeta_3(\zeta_1 - \zeta_2) - K_2(\zeta_1 - \zeta_3)}{\zeta_3(\zeta_3 - \zeta_2)} \right\} e^{-\zeta_2 t/\tau} \\
 & + \left\{ \frac{(\zeta_1 - \zeta_3)(K_2 - \zeta_3)}{\zeta_3(\zeta_3 - \zeta_2)} \right\} e^{-\zeta_3 t/\tau} \quad (23b)
 \end{aligned}$$

It is of interest to note that the decay of load in the prestressed anchor-circular rigid plate system is of a form similar to that which was derived for the problem of the rigid spheroidal anchor embedded in an infinite viscoelastic medium [3]. The rate of decay of the prestress loss is governed by ζ_2 and ζ_3 which occur in the exponential terms of (23b). From (22) it is evident that this decay is governed by factors such as the creep characteristics of the viscoelastic medium, the anchor configuration and the nature of the load distribution in the anchor region.

The unbonded contact between the plate and the viscoelastic medium implies that it is incapable of sustaining tensile tractions. The contact stresses should therefore be evaluated to establish the limits of applicability of the solution (23). The transformed value of the contact stresses at the interface due to the various distributions of the internal anchor load can be obtained by an integration of the result (17) within the appropriate limits. The resulting integrals, however, do not appear to reduce to a closed form solution. The development of tensile tractions at the interface can, however, be investigated by considering the stress distribution that is developed due to the action of the external load and an internal concentrated anchor force, $\bar{P}(s)$. For this particular problem, the transformed value of the compressive contact stress distribution is given by

$$\bar{\sigma}_{zz}(r, 0, s) = \frac{2\bar{G}(s)\bar{w}_0(s)[1 + \bar{T}(r, c, s)]}{\pi[a^2 - r^2]^{1/2} [\{1 - C_1\}\{1 - \bar{v}(s)\} - C_2]} \quad (24)$$

where

$$C_1 = \frac{2}{\pi} \tan^{-1} \left(\frac{a}{c} \right); \quad C_2 = \frac{ac}{\pi(a^2 + c^2)} \quad (25)$$

Inversion of (24) gives

$$\begin{aligned}
 \sigma_{zz}(r, 0, t) = & \frac{4G_0 w_0^*}{\pi[a^2 - r^2]^{1/2}} \\
 & \times \left[\frac{g_2 - g_3 + K_3(1 + g_1 + 2g_3)}{K_3\{K_3(1 - C_1) - C_2\}} \right] N(t) \quad (26)
 \end{aligned}$$

where

$$\begin{aligned}
 N(t) = & e^{-\zeta_2 t/\tau} + \frac{\chi_1}{\zeta_2} \{1 - e^{-\zeta_2 t/\tau}\} + \frac{\chi_2}{K_1} \{1 - e^{-K_1 t/\tau}\} \\
 & + \frac{\chi_3}{v_2} \{1 - e^{-v_2 t/\tau}\} \quad (27)
 \end{aligned}$$

and all the parameters occurring in (26) and (27) are defined in the Appendix 1.

NUMERICAL RESULTS

The analytical results presented for the relaxation of prestress in the plate-anchor system [(23)] are evaluated for a range of viscoelastic material parameters representative of certain typical geological materials (Table 1). In addition to the viscoelastic properties of the halfspace region the other variables include the length and depth of location of the anchor region together with the load distribution in the anchor region. Only the constant and linear distributions of anchor load are considered for purposes of numerical evaluation. The non-dimensional values for both the anchor length (l) and anchor depth (d) are assigned values of 1, 5 and 10. The contact stress at the interface due to a concentrated internal force (26) has been evaluated in order to investigate the possible occurrence of tensile tractions at the interface for all $t > 0$. It is found that for the geological materials listed in Table 1 no tensile stresses are developed at the interface (for all $0 < t < \infty$) provided d is greater than approximately 0.98. This critical value would then set a realistic limit for the depth of location of an anchor region for maximum long term effectiveness. The decay of prestress with time which occurs in anchors located in the various geological materials is illustrated in Figs. 2–10. These indicate the manner in which the creep loss in the pre-tensioned anchor is influenced by the length and depth of location of the anchor region. It is of interest to note that for the highly

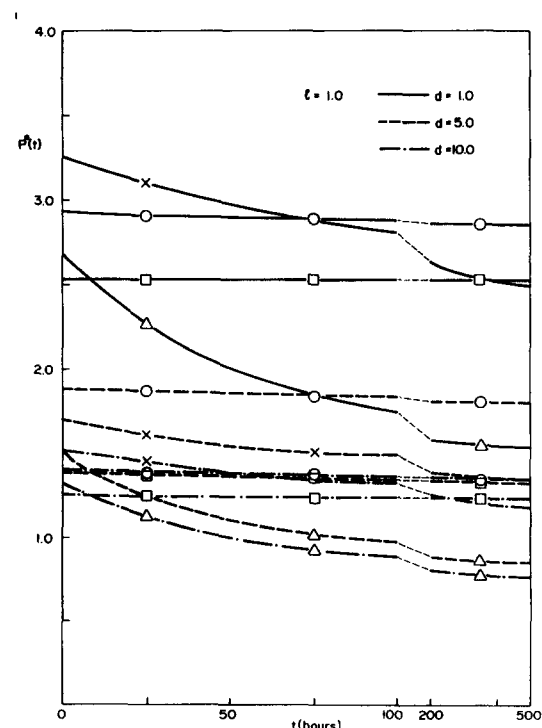


Fig. 2. Load relaxation behaviour of anchor—anchor load distribution constant.

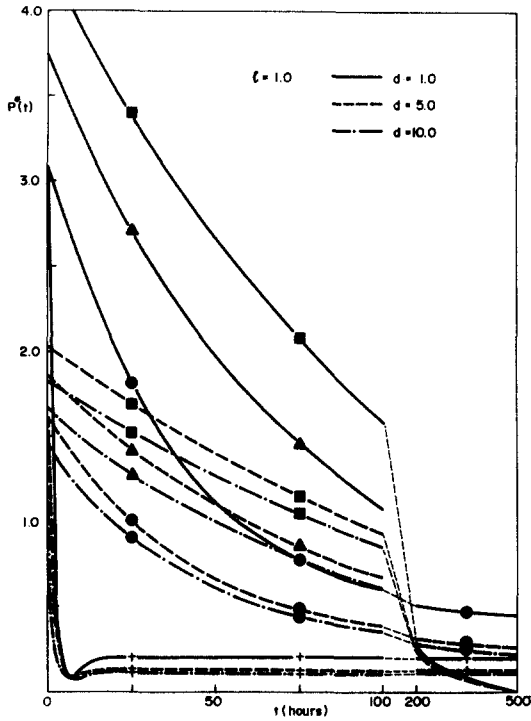


Fig. 3. Load relaxation behaviour of anchor-anchor load distribution constant.

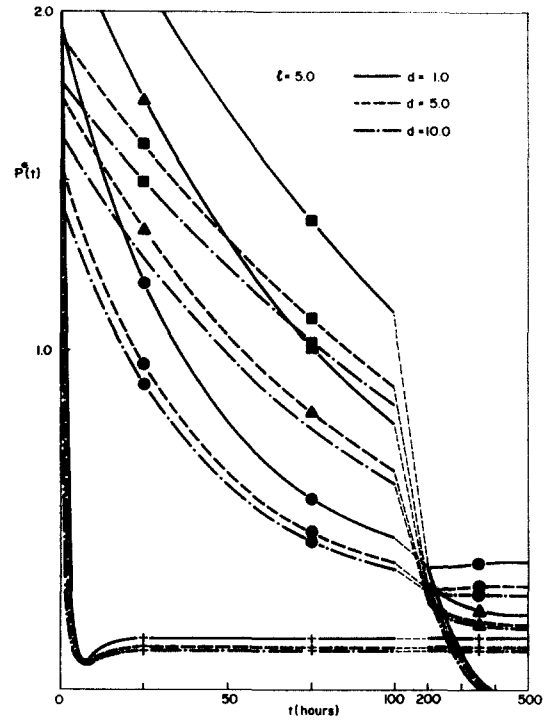


Fig. 5. Load relaxation behaviour of anchor-anchor load distribution constant.

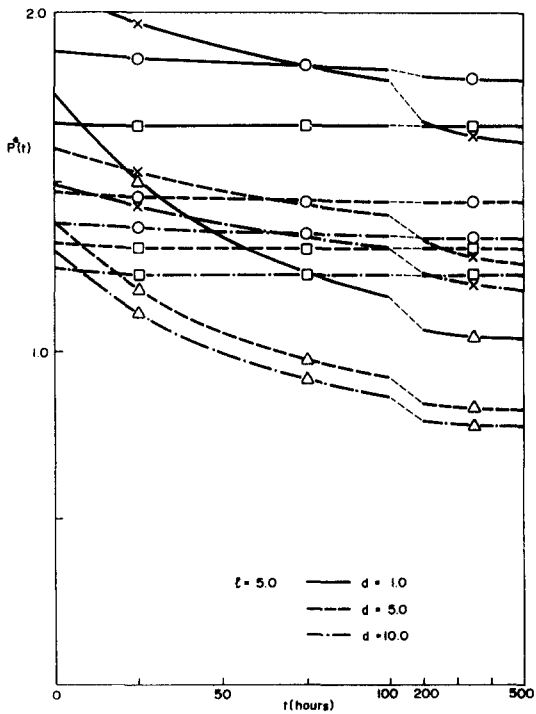


Fig. 4. Load relaxation behaviour of anchor-anchor load distribution constant.

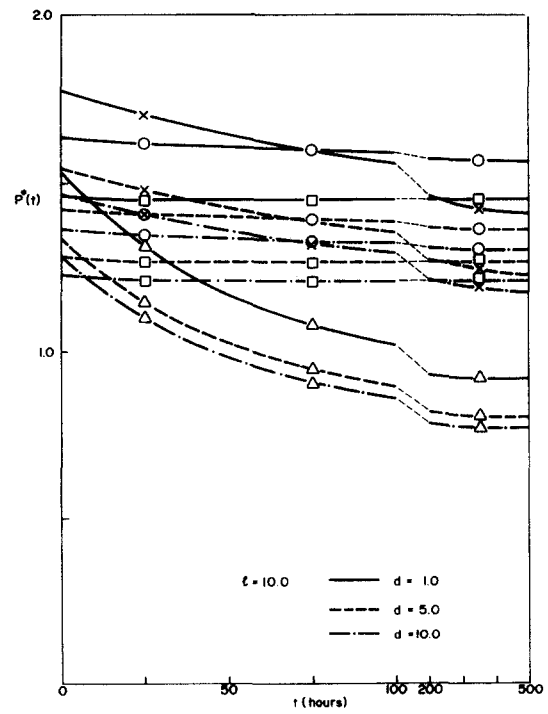


Fig. 6. Load relaxation behaviour of anchor-anchor load distribution constant.

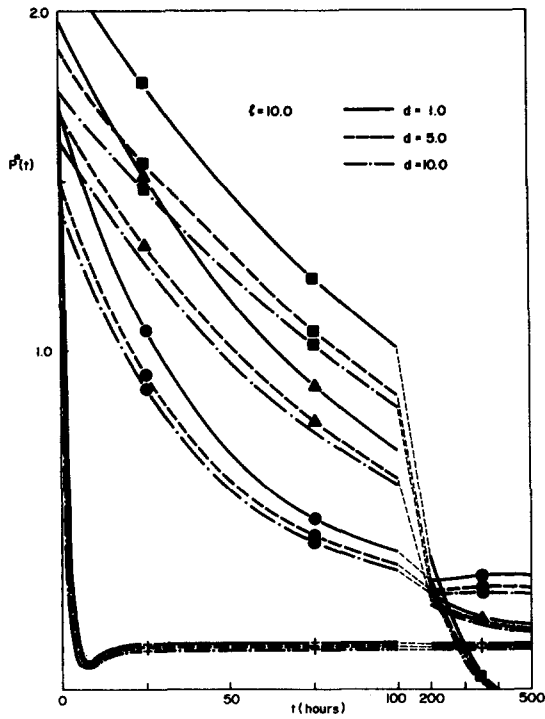


Fig. 7. Load relaxation behaviour of anchor-anchor load distribution constant.

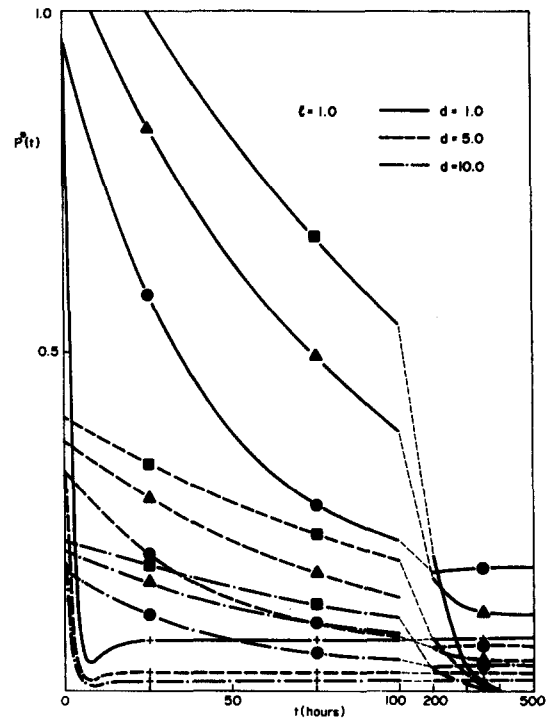


Fig. 9. Load relaxation behaviour of anchor-anchor load distribution linear.

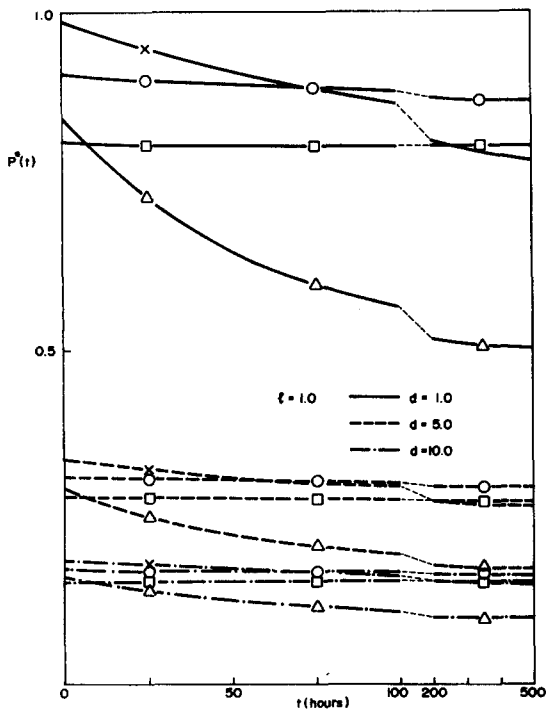


Fig. 8. Load relaxation behaviour of anchor-anchor load distribution linear.

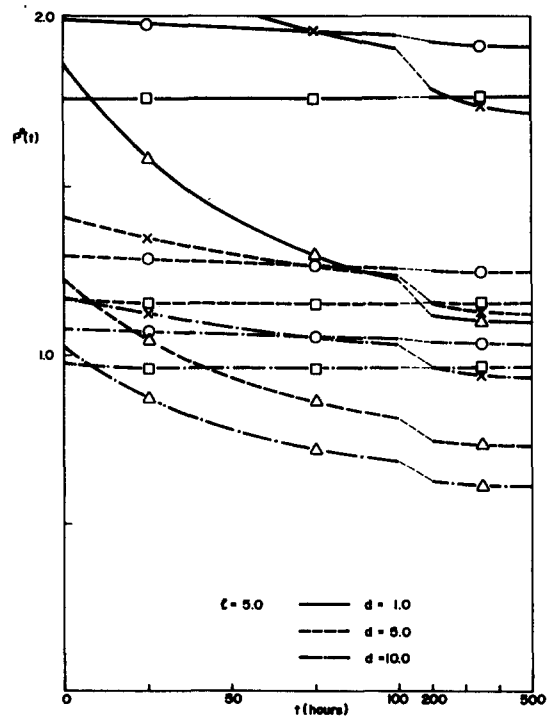


Fig. 10. Load relaxation behaviour of anchor-anchor load distribution linear.

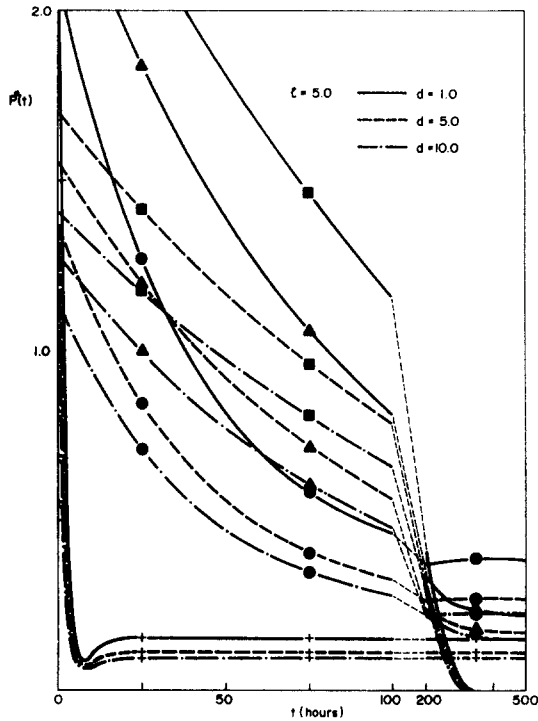


Fig. 11. Load relaxation behaviour of anchor-anchor load distribution linear.

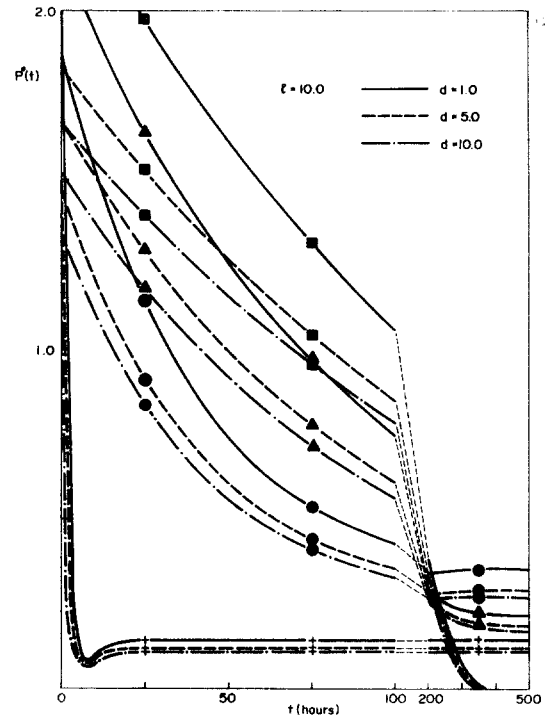


Fig. 13. Load relaxation behaviour of anchor-anchor load distribution linear.

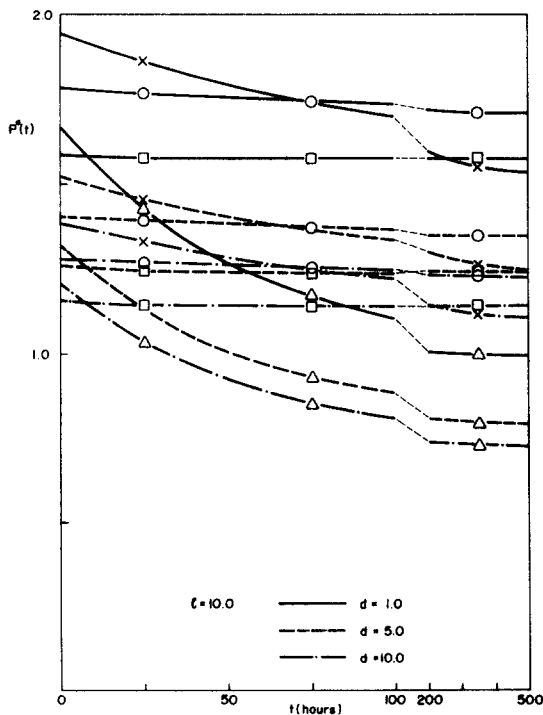


Fig. 12. Load relaxation behaviour of anchor-anchor load distribution linear.

creep susceptible rocksalt and for concrete the decay of prestress is not monotonic. The nature of the load distribution has a significant influence on the initial load developed in the anchor rod and only a moderate influence on the rate of load relaxation.

Acknowledgement—The work described in this paper was supported in part by a research grant awarded by the National Research Council of Canada.

Received 31 October, 1978; in revised form 19 April, 1979.

REFERENCES

1. Lang T. Theory and practice of rock bolting. *Trans. Am. Inst. Min. Metall. Engrs. Min. Div.* **223**, 333-348 (1962).
2. Gosschalk E. M. & Taylor R. W. Strengthening of Muda Dam foundations using cable anchors. In *Proc. 2nd Cong. Int. Soc. Rock Mech., Beograd Vol 3*, pp. 205-270. 'Jaroslav Cerni' Institute for the Development of Water Resources, Belgrade (1970).
3. Selvadurai A. P. S. The time dependent response of a deep rigid anchor in a viscoelastic medium. *Int. J. Rock Mech. Min. Sci. & Geomech. Abstr.* **15**, 11-19 (1978).
4. Harding J. W. & Sneddon I. N. The elastic stresses produced by the indentation of the plane surface of a semi-infinite elastic solid by a rigid punch. *Proc. Camb. Phil. Soc.* **41**, 15-26 (1945).
5. Sneddon I. N. *Fourier Transforms*, McGraw-Hill, New York (1951).
6. Green A. E. On Boussinesq's problem and penny-shaped cracks. *Proc. Camb. Phil. Soc.* **45**, 251-257 (1949).
7. Green A. E. & Zerna W. *Theoretical Elasticity*, Clarendon Press, Oxford (1968).
8. Collins W. D. Some axially symmetric stress distributions in elastic solids containing penny shaped cracks. I. Cracks in an infinite solid and a thick plate. *Proc. R. Soc. Ser. A* **203**, 359-386 (1962).
9. Mindlin R. D. Force at a point in the interior of a semi-infinite solid. *Physics*, **7**, 195-202 (1936).
10. Flugge W. *Viscoelasticity*, p. 97. Blaisdell, MA (1967).

APPENDIX 1

The anchor region is located at a depth ad below the surface of the viscoelastic halfspace. The total anchor load P is distributed uniformly, linearly or parabolically over a length al (Fig. 1). The form of these anchor load distributions are assumed to remain constant for all $t > 0$. In the following we list the functions $A_i(l, d)$, ($i = 1, 2$) which characterize the various anchor load distributions.

(i) *Constant load intensity*

$$A_1(l, d) = \frac{2}{\pi l} I_1(l, d); \quad A_2 = \frac{1}{\pi l} I_2(l, d)$$

where

$$I_1(l, d) = (l + d) \tan^{-1} \left(\frac{1}{l + d} \right) - d \tan^{-1} \left(\frac{1}{d} \right) + \frac{1}{2} \ln \left[\frac{1 + (l + d)^2}{1 + d^2} \right]$$

$$I_2(l, d) = \frac{1}{2} \ln \left[\frac{1 + (l + d)^2}{1 + d^2} \right]$$

(ii) *Linear load intensity*

$$A_1(l, d) = \frac{4}{\pi l^2} \{ (l + d) I_1(l, d) - I_3(l, d) \}$$

$$A_2(l, d) = \frac{2}{\pi l^2} \{ (l + d) I_2(l, d) - I_4(l, d) \}$$

where

$$I_3(l, d) = \frac{1}{2} \left\{ l + [1 + (l + d)^2] \tan^{-1} \left(\frac{1}{l + d} \right) - (1 + d^2) \tan^{-1} \left(\frac{1}{d} \right) \right\}$$

$$I_4(l, d) = l - \tan^{-1}(l + d) + \tan^{-1}(d)$$

(iii) *Parabolic load intensity*

$$A_1(l, d) = \frac{6}{\pi l^3} \{ (l + d)^2 I_1(l, d) - 2(l + d) I_3(l, d) + I_5(l, d) \}$$

$$A_2(l, d) = \frac{3}{\pi l^3} \{ (l + d)^2 I_2(l, d) - 2(l + d) I_4(l, d) + I_6(l, d) \}$$

where

$$I_5(l, d) = \frac{(l + d)^3}{3} \tan^{-1} \left(\frac{1}{l + d} \right) - \frac{d^3}{3} \tan^{-1} \left(\frac{1}{d} \right) + \frac{l}{6} (l + 2d) - \frac{1}{6} \ln \left[\frac{1 + (l + d)^2}{1 + d^2} \right]$$

$$I_6(l, d) = \frac{l}{2} (l + 2d) - \frac{1}{2} \ln \left[\frac{1 + (l + d)^2}{1 + d^2} \right]$$

In equation (25) g_i ($i = 1, 2, 3$) are functions of r and c given by

$$g_1 = -\frac{2}{\pi} \tan^{-1} \left(\frac{a}{c} \right)$$

$$g_2 = \frac{-ac}{\pi(a^2 + c^2)} + \frac{ac^3}{\pi(r^2 + c^2)^2} \left\{ 1 + \frac{\{2a^2 + c^2 - r^2\}}{(a^2 + c^2)} + 3 \sqrt{\frac{a^2 - r^2}{r^2 + c^2}} \tan^{-1} \sqrt{\frac{a^2 - r^2}{r^2 + c^2}} \right\}$$

$$g_3 = \frac{ac}{\pi(r^2 + c^2)} \left[1 + \sqrt{\frac{a^2 - r^2}{r^2 + c^2}} \tan^{-1} \sqrt{\frac{a^2 - r^2}{r^2 + c^2}} \right]$$

Also, the parameters χ_i ($i = 1, 2, 3$) are given by the solution of

$$\begin{bmatrix} \chi_1 \\ \chi_2 \\ \chi_3 \end{bmatrix} = \begin{bmatrix} 1 & 1 & 1 \\ (K_1 + v_2) & (\zeta_2 + v_2) & (K_1 + \zeta_2) \\ K_1 v_2 & \zeta_2 v_2 & K_1 \zeta_2 \end{bmatrix}^{-1} \begin{bmatrix} \zeta_1 + v_1 + K_2 - \zeta_2 - v_2 \\ \zeta_1 K_2 + v_1 K_2 + \zeta_1 v_1 - K_1 v_2 \\ \zeta_1 v_1 K_2 \end{bmatrix}$$

and v_1 and v_2 are given by

$$v_1 = \frac{K_1(g_2 - g_3) + K_1 K_3(1 + g_1 + 2g_3)}{g_2 - g_3 + K_3(1 + g_1 + 2g_3)}$$

$$v_2 = \frac{K_1 K_3(1 - C_1) - K_2 C_2}{K_3(1 - C_1) - C_2}$$